JOURNAL OF MATERIALS SCIENCE 26 (1991) 6722–6728

Nitride and carbonitride layers of titanium formed under high energy ion irradiation

W. ENSINGER*
Institut für Physikalische Chemie, Universität Heidelberg, 6900 Heidelberg, Germany
J. M. MAYNE
Inorganic Materials Department, Government Industrial Research Institute, Osaka, Ikeda, 563 Japan

Titanium nitride and carbonitride films were formed by evaporating titanium while simultaneously irradiating with energetic nitrogen ions in an atmosphere of N_2 and $C_2H_2 + N_2$, respectively. The physical and chemical properties, such as composition, purity, hardness, adhesion and corrosion resistance behaviour, were examined with respect to the process parameters such as nitrogen ion current density and the process pressure of the reactive gases. Nitride and carbonitride phases can be obtained over a wide range of process parameters. Oxygen contamination strongly depends on the ion current density. Deposits of TiN were prepared with hardness values of up to 2800 kgmm^{-2} and adhesion values of up to 15 N critical load in the scratch test. For TiCN the values were 4000 kgmm^{-2} and 10 N. Even a thin layer of only 1 μm of either TiN or TiCN reduced the corrosion rate of stainless steel in sea water by about an order of magnitude over a period of one month.

1. Introduction

In order to synthesize binary and ternary ceramic compounds like metal nitrides or carbonitrides, the non-metallic component may be introduced into the metal lattice in different ways. The direct method is to implant the non-metallic component using highly energetic ions. Ions with energies of several keV penetrate the surface of a solid and come to rest in the host lattice. Usually it is not necessary for the bulk material to be at a high temperature. Using oxygen or nitrogen ions, oxides and nitrides can be formed [1]. This process of thin layer ceramic formation is suitable for converting the surface region of a metal into a hard material.

If the substrate and the ceramic coating are required to be of different materials the substrate is first coated with the metallic component which is then converted into the desired ceramic by ion implantation (ion beam mixing). Both methods are shown schematically in Fig. 1.

These techniques offer some advantages over other coating methods, e.g., low process temperature and high controllability of the ion beam process. The major disadvantage is that the thickness is limited. The thickness of the coating or the converted region depends on the entrance depth of the ions which is determined by the ion energy. With the current equipment, energies of several hundred keV are available resulting in ion penetration depths usually below 1 μm.

To overcome this problem without losing the benefits of the ion beam technique, both metallic coating and non-metallic incorporation are carried out simultaneously (Fig. 1c). Metal atoms are evaporated or sputtered and condensed on to the substrate and at the same time are irradiated with the non-metal ions. The coating compound is formed dynamically without thickness limitation. This technique is known as dynamic ion beam mixing [2, 3]; ion beam enhanced, activated or assisted deposition [4–8] as well as other terms [9]. For this paper, the term ion beam assisted deposition (IBAD) will be used. If another component, a reactive gas, is involved, the process is called reactive ion beam assisted deposition (RIBAD) (Fig. 1d).

In this study, titanium was evaporated and simultaneously irradiated with nitrogen ions to form titanium nitride (IBAD). In a further experiment, acetylene was introduced into the system as a third component which resulted in the formation of the ternary hard material titanium carbonitride (RIBAD).

2. Experimental procedure

Fig. 2 shows a schematic representation of the experimental set-up. The vacuum chamber contains an electron beam gun for titanium evaporation and a hot cathode ion source for generation of the nitrogen beam [10]. Both can be separated from the substrate by means of shutters. The evaporation rate is measured by a quartz crystal monitor. The ion impact rate

* *Present address*: Material Physics Department, Government Industrial Research Institute, Osaka, Ikeda, 563 Japan.

 0022–2461/91 $03.00 + .12 © *1991 Chapman & Hall*

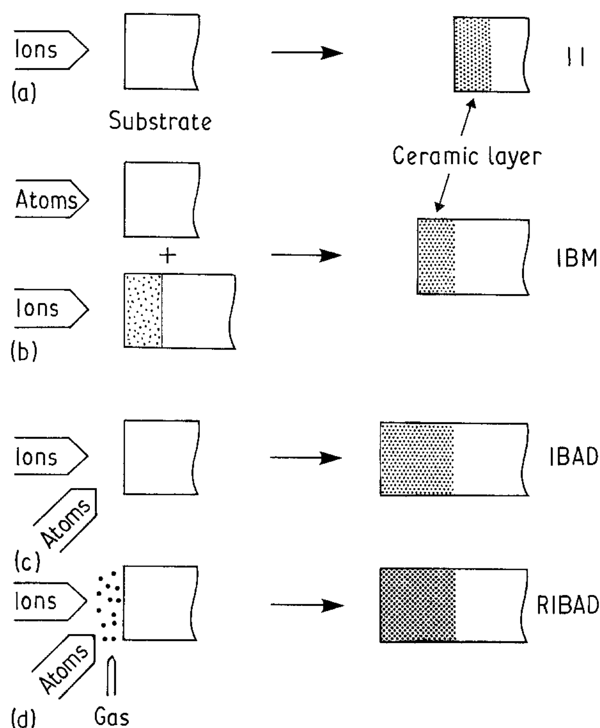

Figure 1 Ion beam surface modification and coating techniques of (a) ion implantation; (b) ion beam mixing; (c) ion beam assisted deposition and (d) reactive ion beam assisted deposition.

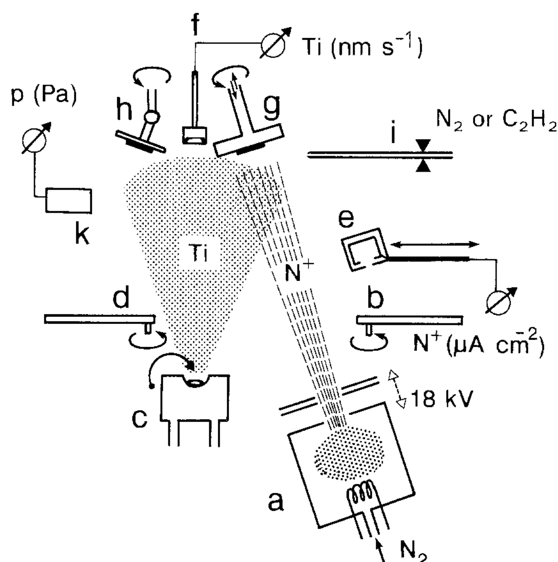

Figure 2 Schematic representation of apparatus for reactive ion beam assisted deposition where a is the ion source for generation of nitrogen beam; b, the ion source shutter; c, the electron beam evaporator; d, the atom beam shutter; e, the ion beam monitor (Faraday cup); f, the condensation rate/thickness monitor (quartz crystal); g, the rotating cooled substrate holder; h, the rotating substrate holder for reference sample; i, the leak valve for reactive gas back-filling and k, the pressure gauge.

is measured with an ion current monitor (Faraday cup) which can be moved into the beam. The sample temperature can be determined with a thermocouple. The samples are mounted with springs onto a rotating cooled copper substrate holder. Another holder is used for reference samples which are not to be irradiated. For reactive ion beam assisted deposition acetylene can be back-filled through a needle valve into the chamber.

The substrates used were polished Si wafers, SiO_2 and AISI 304 stainless steel plates of dimensions 20×20 mm. The purity of the titanium and acetylene used was 99.9% and of the nitrogen 99.999%. The samples were cleaned with trichloroethylene in an ultrasonic bath prior to use. After mounting on the substrate holder a jet of dry nitrogen was blown over the samples to remove dust particles. After pumping the vacuum chamber down to a pressure of $8\text{–}10 \times 10^{-5}$ Pa, titanium was melted and outgassed with the electron beam and the ion gun started. The process pressure in the chamber was $1\text{–}12 \times 10^{-3}$ Pa resulting from outgassing of the ion source or back-filling the reactive gas into the chamber. After reaching stable conditions the substrate was irradiated for several minutes prior to deposition in order to clean it by sputtering.

Evaporation rates ranged from 0.1 to 2 nm s^{-1} and ion current densities from 10 to 200 μA cm^{-2}. 18 keV was the usual ion energy used, generated by an 18 kV acceleration voltage, although in some cases the ion energy was as low as 6 keV. Process temperatures ranged from 50 to 250 °C depending on the ion current. Coating thicknesses ranged from 0.1 to 3 μm. The composition of the resulting deposit was examined by Auger electron spectroscopy combined with a 3 keV argon ion sputter etch. The sensitivity factors for quantitative determination of elemental concentrations were obtained from powders of TiN, TiC and TiO_2. The procedure for separating the overlapping Ti and N peaks has been described elsewhere [11].

The microhardness of the coatings was determined with a Knoop indentor with loads from 5 to 20 gf. The direct pull test [12] and the scratch test [13] were used to measure the adhesion of the coating to the steel substrate. In the pull test a 2.5 mm diameter pin was glued to the coating with epoxy cement, and the force to pull off the coating was recorded. In the scratch test a Rockwell C diamond stylus was moved over the coating with an increasing load until the film became detached.

The ability of the coatings to protect against corrosion was determined by immersion in sea water at 25 °C and measuring the weight loss by a microbalance.

3. Results and discussion

The compound films were analysed for composition and purity. Mechanical and chemical properties including hardness, adhesion to substrate and corrosion protection potential were examined.

3.1. Composition and Purity

Fig. 3 shows a typical Auger concentration profile of a titanium nitride layer obtained by nitrogen implantation into a titanium sample or a titanium film on a different substrate. Titanium nitride is not formed in the uppermost surface layers as the energetic nitrogen ions have a certain penetration depth. The surface region is titanium enriched and oxidized. After etching away this region titanium nitride appears with an

atomic ratio of Ti:N of about 1:1. Quantitative depth measurement is difficult with Auger electron spectroscopy, where no depth scale is given. However, the average ion range can be calculated with reasonable accuracy. According to TRIM (Transport of Ions in Matter) calculations most of the nitrogen ions which enter titanium with a typical energy of 30 keV are located within a band of 100 nm [14]. Nitride formation is therefore restricted to a shallow thickness.

Dynamic implantation during film growth (IBAD) overcomes this problem. In the static process ions are implanted into the substrate until the desired concentration is achieved or the saturation level is reached. In the dynamic process the situation is more complicated. The ratio of condensing atoms to impinging ions has to be adjusted. A mismatch cannot lead to the desired composition. As a first approach for the formation of stoichiometric titanium nitride, i.e. equal numbers of titanium and nitrogen atoms in the lattice, the ratio of the condensing titanium atoms to impacting nitrogen ions was held at 1:1. If both atoms and ions remain in the condensing film, 1:1 stoichiometry should be achieved. Accordingly the atom:ion ratio has to be changed if some other Ti:N ratio is required (Table I formula 'a'). In the IBAD process the rate of evaporating atoms and of impacting ions are independent of each other, so it is possible to select and control these parameters over a wide range, unlike plasma techniques.

This basic assumption does not take into account the various physical processes which take place such as sputtering, ion reflection, diffusion and desorption. Experiments show that with a 1:1 ratio of titanium atoms to nitrogen ions according to the above mentioned assumption, a coating of stoichiometric TiN is indeed formed, within the limits of experimental error. A titanium evaporation rate of 0.2 $nm\,s^{-1}$ and an ion current density of 120 $\mu A\,cm^{-2}$ ($Ti:N^+ = 1$) yielded a film of composition $TiN_{1.1}$. Increasing the Ti atom:N^+ ion ratio from 1:1 to 3:1 is expected to produce films with a much lower nitrogen content. Fig. 4 shows the composition profile for such a film (0.16 μm on Si). The nitrogen content of 40 at % is much higher than expected. Clearly the excess must come from a source other than the ion beam. The nitrogen molecules in the residual atmosphere in the vacuum chamber must be incorporated into the film with the highly reactive titanium atoms.

The ion source operates under a pressure much higher than the background pressure. It releases nitrogen gas into the chamber increasing the pressure by about one order of magnitude. Thus sufficient nitrogen molecules are present to adsorb on to the freshly deposited titanium surface and react. Hence the composition of the compound layer depends on both the ion current and the gas pressure (Table I formula 'b'). If the nitrogen supplied by the beam and the residual gas is not sufficient the resulting layers have a nitrogen content too low to form a pure TiN phase. For a titanium evaporation rate of 1 $nm\,s^{-1}$

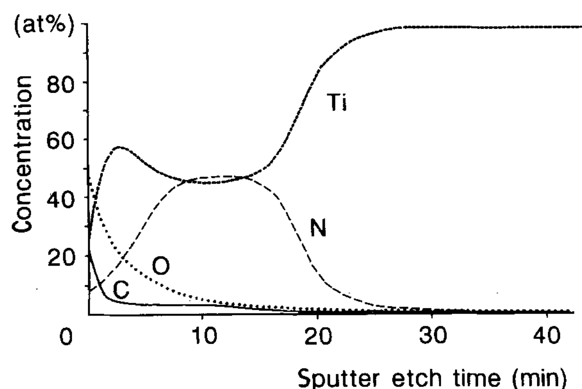

Figure 3 Auger electron composition profile of a Ti sample implanted with nitrogen ions.

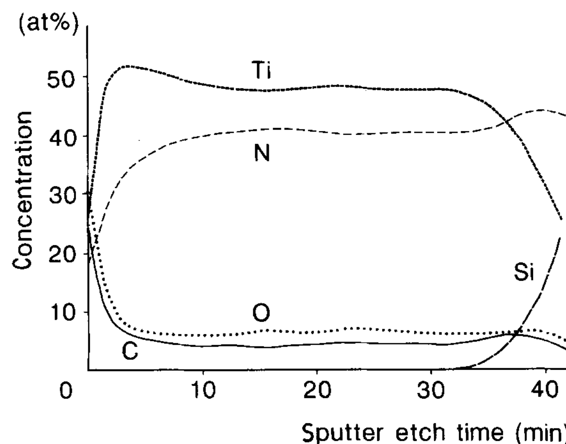

Figure 4 Auger electron composition profile of an IBAD TiN layer (0.16 μm thickness) on Si.

TABLE I Chemical reactions during RIBAD process

Reaction		Atom		Ion		Residual or back-filled gas		Product
Nitride formation	a	Ti	+	aN			→	TiN_x
	b	Ti	+	aN	+	bN_2	→	TiN_x
Side reactions:								
oxygen,	c	Ti			+	$aH_2O + bO_2$	$\xrightarrow[-H]{}$	TiO_x
carbon,	d	Ti			+	aC_mH_n (CO_2, $C_mH_nO_o$)	$\xrightarrow[-H]{}$	TiC_x
hydrogen incorporation	e	Ti			+	X_mH_n	→	$TiH_x(X_y)$
Carbonitride formation	f	Ti	+	aN	+	$bN_2 + cC_2H_2$	$\xrightarrow[-H]{}$	TiC_xN_y

and an ion current density of 20 μA cm^{-2} X-ray analysis showed a mixture of phases of TiN, Ti_2N and α-Ti. Similar results have been obtained elsewhere [15, 16].

The properties of the film depend not only on the nitrogen content but also on the oxygen and carbon. The composition profile in Fig. 4 shows an oxygen content of 6–7 at % and a carbon content of around 4–5 at %. Although nitrogen is the major constituent the residual gas also contains other reactive species, mainly water, oxygen and hydrocarbons. The latter comes from the oil in the vacuum pumping system. Oxygen comes from the leakage of the vacuum chamber and desorption from the chamber walls, especially during operation of the electron beam evaporator and the ion source when parts of the chamber are heated. Often these species react preferentially with titanium, resulting in considerable contamination of the deposited layers. Some of the reactions which take place are listed in Table I formulae 'c–e'.

The ion beam has a marked influence on contamination. In Fig. 5 the composition of two layers is compared. They are formed simultaneously, however, one experiences ion bombardment and the other does not. Despite the high partial pressure of nitrogen the film deposited without the influence of the ion beam contains almost as much oxygen as nitrogen. Oxidation is thermodynamically and kinetically more favourable than nitridation. Under ion beam irradiation the oxygen content is dramatically reduced. One reason might be that enhanced nitrogen reactivity under ion irradiation as ions bring a much higher energy into the system than the chemical bonding forces. The stably-bonded nitrogen can react more easily under such extreme conditions. Another reason may be the removal of oxygen from the surface by sputtering.

Fig. 6 shows quantitatively how the oxygen content depends on the ion beam. Even at low nitrogen ion current densities the oxygen content is greatly reduced. As the current density is increased the oxygen content is further reduced, but with decreasing efficiency. Some oxygen contamination can always be found in the film even at very high current densities. To avoid this problem water and oxygen have to be eliminated from the chamber by baking and by improved constructural means such as better sealing and a stronger pump. Conversely carbon contamination is not reduced by ion irradiation. In all cases there was a slight enhancement of the carbonization under the influence of the beam, although this effect is minor compared with the marked reduction in oxidation. These side reactions can be used to introduce a third component in the film. Deliberately back-filling the chamber with acetylene means that carbon partly substitutes for nitrogen in the film (Table I formula 'f').

Fig. 7 shows the composition profile of the first 150–200 nm of a 1 μm thick film on Si. The average composition was: Ti: 48 at %; C: 28 at %; N: 20 at % and O: 4 at %. Titanium carbide and nitride are isomorphous having the NaCl structure and a very similar lattice parameter. Nitrogen and carbon occupy the octahedral interstitial positions in an f.c.c. Ti lattice. The carbide and nitride are completely miscible. It is therefore possible to form carbonitrides by RIBAD simply by substituting a part of the residual nitrogen gas by a carbon containing gas.

The RIBAD formation of carbonitrides is comparable to plasma techniques [17] although there are

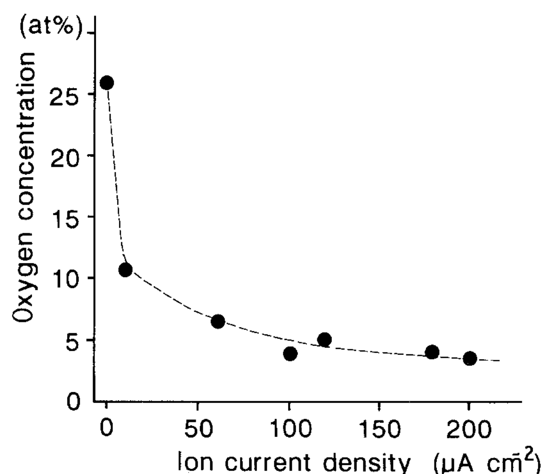

Figure 6 Dependence of oxygen concentration in TiN films on nitrogen ion current density.

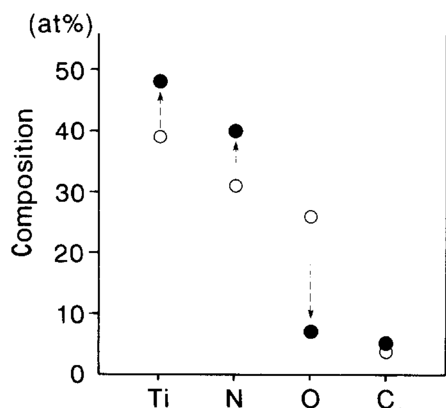

Figure 5 Comparison of composition of evaporated Ti films of IBAD with simultaneous nitrogen ion bombardment (●) and evaporation without simultaneous nitrogen ion bombardment (○).

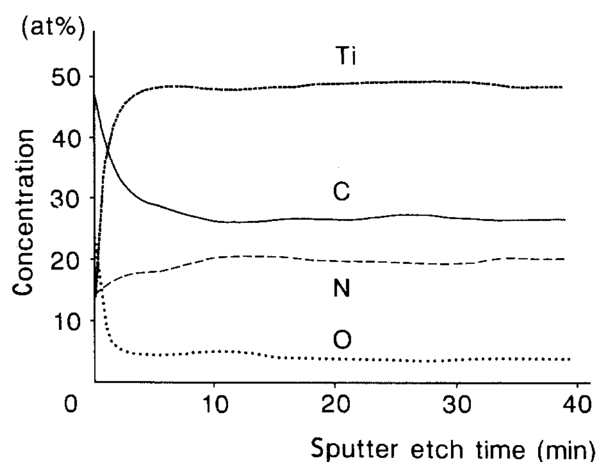

Figure 7 Auger electron composition profile of a TiCN layer on Si.

differences. The plasma is formed by a gas mixture e.g. nitrogen and ethylene. Therefore the ethylene ions and fragments or reaction products which impinge on the substrate have high energies. In RIBAD the nitrogen ions have high energies and the hydrocarbon molecules only thermal energies. Hydrogen cannot be detected by Auger spectroscopy. Judging by plasma techniques only a very small amount should be incorporated. Most of the hydrogen liberated by the process is expected to combine with molecules and desorb from the surface. Special techniques such as nuclear reaction analysis could be used in future for hydrogen analysis.

3.2. Mechanical properties

Metal nitrides and carbides are extremely hard. Hardness values cited for TiN coatings are from 340 to 3800 $kgmm^{-2}$ [18, 19]. The hardness depends on both the preparation technique and process parameters. Fig. 8 shows the hardness value ranges for titanium nitride and carbonitride films compared with the bulk material. Nitrogen implantation leads to a slight but significant increase in hardness. This shows that the shallow layer formed must be considerably harder than the unirradiated bulk titanium. The IBAD TiN films on quartz showed hardness values in the range 1400–2800 $kgmm^{-2}$. Bulk TiN has a hardness of approximately 2000 $kgmm^{-2}$ [20]. Hardness values equivalent or higher to those of the bulk material may be obtained if the appropriate process parameters are selected.

It is important to realise that the hardness measurements on thin films often lead to lower values. The indentor may penetrate too deeply into the layer so that the substrate hardness affects the result. The real value may be higher than recorded. At least formation of hard materials is verified and trends are observed. Fig. 9 shows the dependence of the hardness on the nitrogen ion current density. The hardness increased with increasing current density until a maximum of about 2800 $kgmm^{-2}$ was reached. Increasing the current density further, decreased the hardness. The hardness depends on many factors such as composition, density and structure. At lower ion current densities, like Ti atom:N^+ ion ratio of 10:1, it is possible that less nitrogen has been incorporated. The α-phase of titanium may remain leading to a softer film. Higher current densities lead to higher nitrogen content, higher density, structural changes and changes in crystal orientation [3, 4, 16] and thus to harder films. Increasing the ion current further leads to a downturn in the hardness curve which may be due to structural changes. Too much nitrogen may lead to blistering which weakens cohesion and reduces hardness. Substitution of nitrogen by carbon greatly increases hardness. Bulk TiC is about 50% harder than bulk TiN [20]. Carbon forms stronger bonds with titanium than nitrogen. Cohesion is enhanced, and the melting point and hardness increase. Hardness values for carbonitrides are inbetween nitrides and carbides. Using RIBAD, however, carbonitride films with hardness values of above 4000 $kgmm^{-2}$ could be obtained. This is higher than the hardness of pure bulk TiC.

The amount of carbon substitution depends on the number of carbon atoms available for reaction and hence on the partial pressure of the hydrocarbon in the chamber. Fig. 10 shows the dependency of the microhardness on the pressure of acetylene supplied to the machine. Increased pressure results in increased hardness up to values higher than 4000 $kgmm^{-2}$. Of course high hardness is necessary for protection against wear and abrasion. The adhesion of the coating to the substrate is also important. Stainless steel for example is corrosion resistant, but comparatively soft and susceptible to wear. A hard coating considerably enhances its lifetime under wear conditions provided the adhesion is high enough. Adhesion depends on many factors in particular the interface between coating and substrate. Usually a clean, broad interface region yields high adhesion values. The formation of such an interface is favoured by very energetic ions. Ions penetrate into the solid and collide with atoms causing a high degree of atomic motion and hence strong mixing in the target region. As the highly energetic ions have a certain entrance depth, the mixing effect continues to occur even after formation of a coating layer and the interface is already

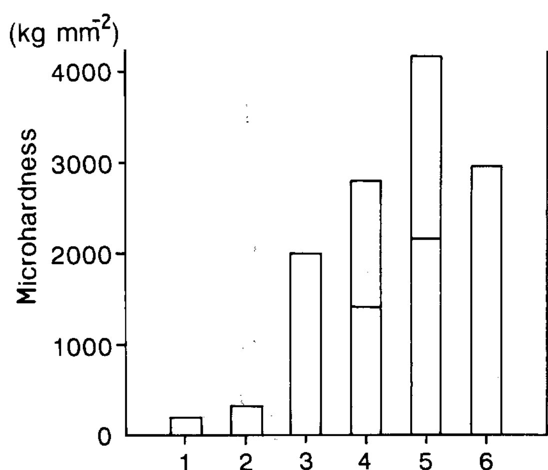

Figure 8 Microhardness of coatings and bulk materials. a: Ti untreated; b: Ti bombarded with nitrogen ions; c: TiN bulk [20]; d: IBAD TiN coating; e: RIBAD TiCN coating; f: TiC bulk [20].

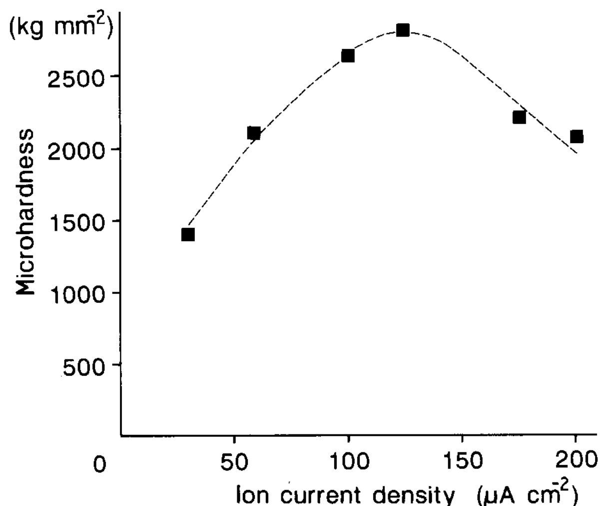

Figure 9 Dependence of microhardness of IBAD TiN films on nitrogen ion current density.

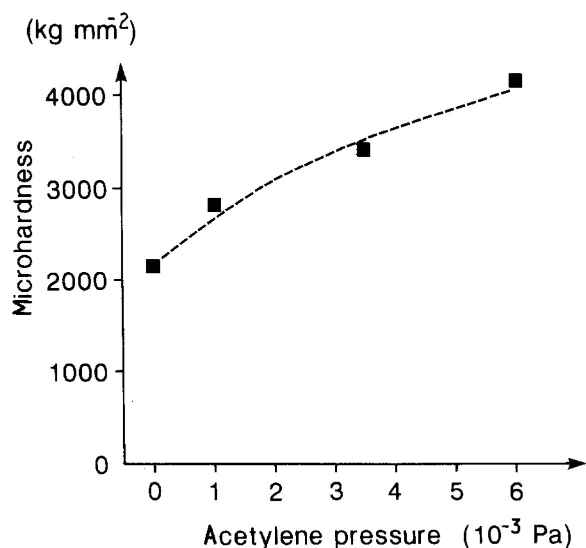

Figure 10 Dependence of microhardness of RIBAD TiCN films on C_2H_2 partial pressure.

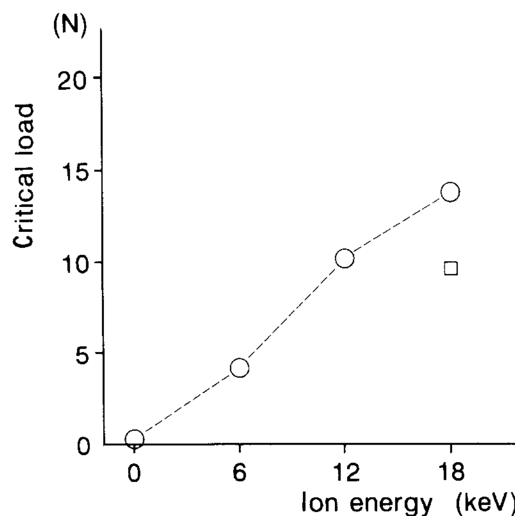

Figure 12 Critical load of scratch-test against nitrogen ion energy for TiN and TiCN films on stainless steel where ○ is TiN and □ is TiCN.

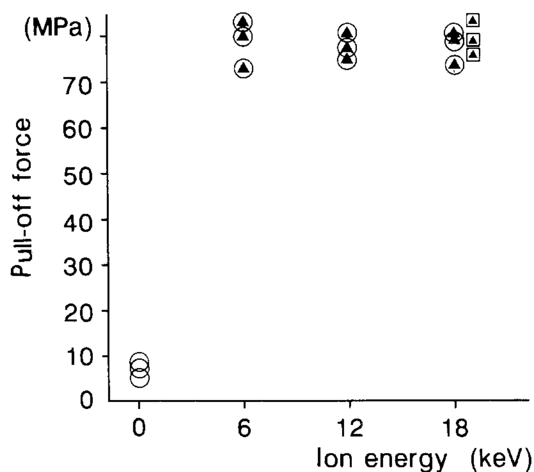

Figure 11 Pull-off force of direct pull-off test against nitrogen ion energy for TiN and TiCN films on stainless steel where ○ is TiN; □ is TiCN and ▲ is failure of glue.

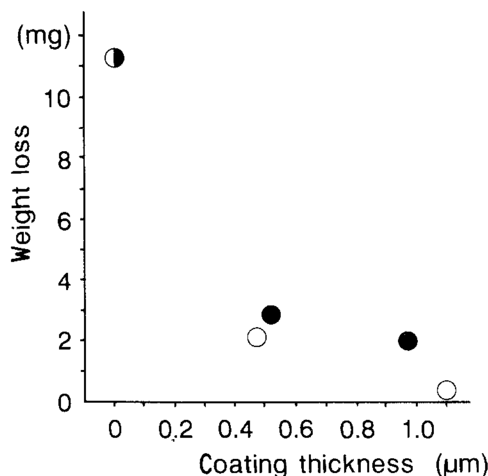

Figure 13 Weight loss of TiN and TiCN coated stainless steel samples after 28 days in sea water as a function of coating thickness where ○ is TiN and ● is TiCN.

buried below the surface. The ion energy therefore plays an important role. Figs 11 and 12 show adhesion test results of TiN and TiCN coatings on stainless steel. Three different ion energies were used.

The direct pull-off test gives adhesion values below 10 MPa for a reference sample which was not irradiated i.e., ion energy zero. Applying ions immediately raises the pull-off force by at least one order of magnitude. In all cases the limit of the test at around 80 MPa is reached, which is where the glue itself fails. This test shows that a strong enhancement of adhesion is achieved but for well adhering films only a threshold value can be obtained. The scratch test is a much better method for hard films. In the investigated energy range an almost linear increase in critical load with the ion energy was observed. The adhesive force of the carbonitride formed with ions of 18 keV was considerably lower than the nitride formed at the same ion energy. This may be due to the higher brittleness of the carbonitride. For both nitride and carbonitride the absence of ion irradiation leads to much lower adhesion values. The critical load depends on the coating thickness and process temperature. For thin coatings (less than 2 μm) and low temperatures i.e., below 200 °C, such as those used in IBAD, critical load values in the range 10–15 N represent high adhesion [13, 21, 22].

Unreactive ceramic coatings can protect a substrate material from environmental destruction. Stainless steel is an example of a highly corrosion resistant material but under severe corrosion conditions such as sea water it is susceptible to degradation. The results of some corrosion tests are shown in Fig. 13. AISI 304 stainless steel samples coated with either TiN or TiCN were immersed in sea water for 28 days. AISI 304 contains Cr: 18% and Ni: 8% but almost no Mo, which would render it more resistant to chloride attack. Chloride ions, local pH value changes and oxygen depletion, which can lead to failure of the protecting oxide film, are amongst the causes of corrosion in sea water. The uncoated steel plates lost more than 11 mg during the test. A TiN coating of only 0.5 μm thickness was sufficient to reduce the weight loss to 2 mg. The carbonitride coating is slightly less

effective. The appearance of the coatings did not change during the test but remained bright. The coating itself does not corrode in this medium as was demonstrated by doing the same experiment with a coated quartz plate, which remained completely unchanged. Hence the corrosive loss from the coated steel plates is due to the dissolution of the steel substrate. Solution can enter the coating through micropores, through edges which have a low degree of coverage, and through uncovered patches which were shaded by dust particles during coating. Increasing the thickness of the coating reduces these effects. A TiN coating of 1 μm reduces the weight loss to a few hundred micrograms. The protection afforded by the carbonitride is somewhat lower but it is unclear as to whether this is due to an electrochemical effect of the carbon, lower adhesion or structural reasons.

4. Summary

Formation of TiN and TiCN is possible at low temperatures (below 250 °C) by ion beam assisted deposition. The composition and purity strongly depends on the process conditions such as nitrogen ion current density and process pressure of the reactive gases. For a certain medium range the Ti atom:N^+ ion beam ratio does not markedly affect the final composition of the titanium nitride layer. The residual gas supplies the deficit nitrogen. The oxygen contamination depends on the ion beam current density. Generally a higher current leads to lower oxygen content. The hardness of the deposit strongly depends on the nitrogen ion current density and process pressure of the reactive gases. It is possible to achieve much higher hardness values for the coatings than for the bulk materials. For TiCN films there is approximately 30% increase over the value for the bulk TiC. Adhesion of the coatings to stainless steel is 10–15 N, which is comparable to or higher than results obtained with plasma techniques.

Both TiN and TiCN coatings considerably reduce corrosion of stainless steel in sea water. As the hardness and adhesion values are high and the corrosion resistance of these deposits is good, they may well find applications as coatings for protection against tribological and chemical deterioration. They may be particularly useful for coating stainless steel because adhesion to it is usually very poor.

Acknowledgement

J. Mayne wishes to thank the EEC Commission for Science, Research and Development for financial support under the "Scientific Training Programme, Japan".

References

1. I. H. WILSON in "Ion beam modification in insulators", edited by P. Mazzoldi and G. W. Arnold (Elsevier, Amsterdam, 1987) Ch. 7, p. 245.
2. M. SATOU and F. FUJIMOTO, *Jpn. J. Appl. Phys.* **22** (1983) L171.
3. M. KIUCHI, K. FUJII, T. TANAKA, M. SATOU and F. FUJIMOTO, *Nucl. Instr. Meth. Phys. Res.* **B33** (1988) 649.
4. J. M. E. HARPER, J. J. CUOMO, R. J. GAMBINO and H. R. KAUFMAN in "Ion modification of surfaces", edited by O. Auciello and R. Kelly (Elsevier, Amsterdam, 1984) Ch. 4, p. 127.
5. G. K. WOLF, M. BARTH and W. ENSINGER, *Nucl. Instr. Meth. Phys. Res.* **B37/38** (1989) 682.
6. G. K. HUBLER, *Mater. Sci. Engng* **A115** (1989) 181.
7. G. K. WOLF, *Vacuum* **39**, (1989) 1105.
8. X. LIU, B. XUE, Z. ZHENG, Z. ZHOU and S. ZOU, *Nucl. Instr. Meth. Phys. Res.* **B39** (1989) 185.
9. Y. ANDOH, K. OGATA, H. YAMAKI and S. SAKAI, *Nucl. Instr. Meth. Phys. Res.* **B39** (1989) 158.
10. H. RYSSEL and I. RUGE, in "Ion implantation" (John Wiley, Chichester, 1986) p. 119.
11. D. A. BALDWIN, B. D. SARTWELL and I. L. SINGER, *Appl. Surf. Sci.* **25** (1986) 364.
12. R. JACOBSSON and B. KRUSE, *Thin Solid Films* **15** (1973) 71.
13. A. J. PERRY, *Thin Solid Films* **107** (1983) 167.
14. J. F. ZIEGLER, J. P. BIERSACK and U. LITTMARK in "The stopping and range of ions in solids" (Pergamon Press, New York, 1985).
15. M. KIUCHI, K. FUJII, H. MIYAMURA, K. KADONO and M. SATOU, *Nucl. Instr. Meth. Phys. Res.* **B37/38** (1989) 701.
16. R. A. KANT and B. D. SARTWELL, *Mater. Sci. Engng* **90** (1987) 357.
17. Y. ENOMOTO and K. YAMANAKA, *Thin Solid Films* **86** (1981) L201.
18. J. E. SUNDGREN, *Thin Solid Films* **128** (1985) 21.
19. M. BARTH, W. ENSINGER, A. SCHRÖER and G. K. WOLF, in "Surface Modification Technologies III", edited by T. S. Sudarshan and D. G. Bhat (TMS, Warrendale, PA, 1990) p. 195.
20. L. E. TOTH in "Transition metal carbides and nitrides" (Academic Press, New York, 1971) p. 7.
21. A. J. PERRY, *Thin Solid Films* **81** (1981) 357.
22. P. J. BURNETT and D. S. RICKERBY, *ibid.* **154** (1987) 403.

Received 25 June 1990
and accepted 31 July 1991